ISSN 1063-7834, Physics of the Solid State, 2017, Vol. 59, No. 10, pp. 1906–1912. © Pleiades Publishing, Ltd., 2017.
Original Russian Text © I.K. Razumov, 2017, published in Fizika Tverdogo Tela, 2017, Vol. 59, No. 10, pp. 1885–1891.

METALS

Stabilization of Growth of a Pearlite Colony because of Interaction between Carbon and Lattice Dilatations

I. K. Razumov

Institute of Metal Physics, Ural Branch, Russian Academy of Sciences, Yekaterinburg, Russia

e-mail: rik@imp.uran.ru

Received April 4, 2017

Abstract—The previously proposed model of pearlite transformation develops taking into account the possible interaction between carbon and lattice dilatations arising in austenite near the pearlite colony. The normal stresses caused by the colony stimulate autocatalysis of plates, and tangential stresses promote the stabilization of the transformation front. The mechanism of ferrite branching, which can play an important role in the kinetics of pearlite and bainite transformations, is discussed.

DOI: 10.1134/S1063783417100304

INTRODUCTION

Pearlite transformation in carbon steel [1–3] belongs to the class of eutectoid transformations in which the initial metastable phase undergoes decomposition below the eutectoid temperature T_{eutec} in two new phases according to the scenario of colony growth. In the case of pearlite transformation into steel at $T_{eutec} < 1000$ K, metastable austenite (γ-Fe, fcc lattice) decomposes into ferrite with low carbon solubility (α-Fe, bcc lattice) and cementite containing 25 at % of carbon (θ-phase, orthorhombic lattice); as a result, a regular lamellar structure is usually formed. Eutectoid transformations are also observed in alloys of Zn–Al [4], Cu–Al [5], Au–In [6], etc.

Despite the similarity of pearlite with structures arising in spinodal decomposition (SD) [7], classical SD is impossible in γ-Fe, since the mixing energy of carbon is positive in this phase [8]. Theoretical studies were focused on the study of the steady growth of the pearlite colony with a flat front [9–14], which made it possible, to establish the temperature dependence of the interplate distance $\lambda \approx 1/(T - T_{eutec})$ being in agreement with the experiment. The authors of [11] first formulated a hypothesis, recently confirmed by the phase-field simulation [15], that the steady growth of a pearlite colony is provided by accelerating the carbon diffusion on its front. It was shown in [15] that, in the absence of this acceleration, the ferrite plates rapidly grow into austenite, which is followed with the destruction of the regular structure of a colony. At the same time, Hillert's opinion is cited in [16], according to which it is difficult to expect a significant acceleration of diffusion at the transformation front taking into account the already rapid diffusion in the volume of phases.

The origin of a pearlite colony was discussed qualitatively in [17], where it was noted that between the A_3 and A_{cm} lines of the phase diagram (Fig. 1) extrapolated to the temperature range $T < T_{eutec}$, austenite is oversaturated with respect to both ferrite and cementite. Carbon is pushed out from ferrite, contributing to the nucleation of cementite at the interface with ferrite. In turn, the growth of the nucleus of cementite leads to the carbon depletion of the adjacent region contributing to the nucleation of ferrite. The process can be described in terms of thermo-fluctuational nucleation, and the probability of the nucleation of each phase depends on the local composition.

The paper [19] was first considered the autocatalytic scenario of the decomposition of metastable phases, and the possibility of realizing such a mechanism during pearlite transformation was discussed. This mechanism differs both from the classical spinodal decomposition and thermo-fluctuational nucleation. Its specificity is that with a special phase energy ratio (Fig. 2), the initial phase can be stable with respect to small fluctuations in the composition, but locally loses its stability when it interacts with the transformation products, i.e., in those regions where a change in concentration above the critical one is achieved due to the drift of system to local equilibrium. As a result, one of the products of the transformation stimulates the rapid nucleation of the other, and the decomposition develops according to the colony growth scenario. The autocatalytic nucleation of precipitates at the grain boundary in a model qualitatively simulating pearlite transformation was considered later [15]. A detailed discussion of the autocatalytic mechanism of the decomposition of metastable

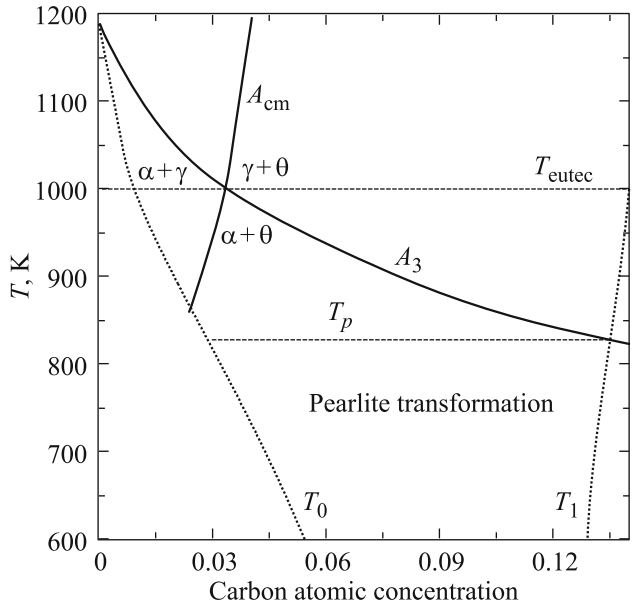

Fig. 1. Diagram of transformations in the Fe–C system constructed in the framework of the model [18] with the refined parametrization (see Appendix). A_3 and A_{cm} are the boundaries of the two-phase regions $\alpha + \gamma$ and $\gamma + \theta$, respectively; T_0 and T_1 are the curves of stability loss of austenite relative to transformations $\gamma \rightarrow \alpha$ and $\gamma \rightarrow \theta$.

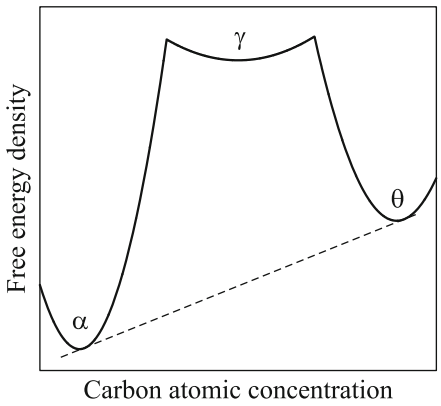

Fig. 2. Free energy of the phases in the pearlite region of the transformation diagram (schematic image). There are no equilibrium conditions α/γ and γ/θ, while maintaining the basic equilibrium α/θ, which leads to the autocatalytic decomposition of the γ phase.

phases is given in the review devoted to the theory of phase transformations in steel [20].

A model of pearlite transformation with the first-principle parametrization was proposed in [18]. The autocatalytic decomposition in this model due to the facilitation of cementite nucleation at the interface of ferrite (the line of stability loss T_1 is shifted to the left, Fig. 1), because of the formation of the metastable intermediate structure (MIS) at the austenite/ferrite interphase, according to the recent ab initio calculations [21]. In contrast to [15], the model [18] uses no assumption of the flat transformation front and the acceleration of diffusion at the front, and autocatalysis was allowed throughout the volume of the material. As a result, decomposition morphologies were observed qualitatively similar to pearlite ones (according to experiments, the colony front need not to be plane [2, 22]). It was the absence of the flat front that facilitated the development of autocatalysis in these calculations and the formation of a lamellar structure. At the same time in the experiments, the lamellae are usually oriented along the normal to the transformation front, which does not completely agree with these calculations.

During the pearlite transformation, the coherence of the lattice at the front of the colony is completely or partially lost [23–25]. Therefore, in most theories it is assumed that the elastic stresses in austenite do not play an important role in the kinetics of the transformation. However, this view of the role of stresses is simplistic. Even in the absence of cooperative atomic displacement, lattice dilatations inevitably arise in the system due to the diffusion of carbon and the difference in the volumes of phases. Concentration stresses caused by a change in the local carbon concentration near the front of the colony were taken into account and led to a noticeable acceleration of the transformation [26]. In addition to the concentration stresses, the stresses caused by the presence of ferrite and cementite act near the colony, which cannot be reduced to the local carbon concentration.

As can be seen from Fig. 3, because of differences in the volumes of austenite, ferrite, and cementite, normal and tangential stresses appear near the ends and in the front of the colony, respectively. Therefore, at the ends of the colony the austenite lattice stretches near ferrite and contracts near cementite. On the contrary, in front of the colony the austenite lattice can stretch near cementite and contract near ferrite. Since the carbon atoms are the centers of dilatation, they diffuse from the compression regions to the stretching regions. Accounting for this circumstance results in the formation of a regular structure and raises the tem-

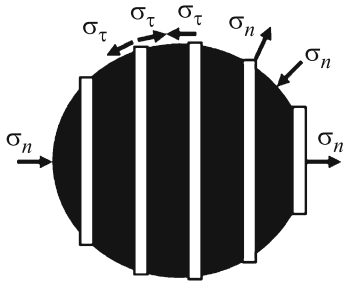

Fig. 3. Normal (σ_n) and tangential (σ_τ) stresses in the vicinity of the pearlite colony (schematic image).

perature of the beginning of autocatalysis, herewith the lamellae are oriented along the normal to the front of the colony in agreement with the experiment.

FORMULATION OF MODEL

We write the Ginzburg–Landau free energy functional in the form

$$F = \int\left(f_{\text{eff}}(c,T) + \frac{k_c}{2}(\nabla c)^2 \right) d\mathbf{r} + F_{\text{el.in}}, \qquad (1)$$

where $F_{\text{el.in}}$ is the energy of the deformation interaction of carbon with the stresses created by the growing colony; $f_{\text{eff}}(c,\ T) = \min\{f_\alpha(c,\ T), f_\gamma(c,\ T), f_\theta(c,\ T)\}$ is the effective free-energy density of the unstressed state, which depends on the local carbon concentration and temperature; $f_{\gamma(\alpha,\ \theta)}(c,\ T)$ are local densities of the free energy of austenite (ferrite, cementite) calculated similarly to the model [18, 20, 27]; k_c is the parameter that determines the width of the interface. The determination of $f_{\text{eff}}(c,\ T)$ assumes a rapid reorganization of the lattice, so that a phase with the lowest free energy is always observed at a given point in space.

Let us describe the main provisions of the approach used [18, 20, 27]. The energies of the α and γ phases in the presence of carbon (or without it) were calculated ab initio for the paramagnetic and ferromagnetic states. The energies of these phases at intermediate temperatures were obtained in agreement with the Oguchi model for the temperature dependence of the spin correlator [28]. The magnetic entropy is taken into account using the Gelman–Feynman theorem [29]. The carbon configuration entropy takes into account that the carbon atoms in the α-phase are distributed over three sublattices of the octahedral interstitial sites, and in the γ-phase can occupy only one-fourth of the octahedral interstitial sites [30]. The temperature dependence of the free energy of stoichiometric cementite is taken from CALPHAD [31] or ab initio calculations [32]. The concentration dependence of cementite energy is selected in an effective form [18] ensuring the realization of the $\gamma \to \theta$ transition (the condition of loss of stability) at concentrations $c = 0.12$–0.15, i.e., far from the stoichiometric composition of cementite. The physical basis for this choice is the probable appearance of the metastable intermediate structure (MIS) at the austenite/ferrite interface facilitating the transition in accordance with ab initio calculations [21], and also the preference for the formation of cementite at the interface with ferrite due to elastic stresses. The parametrization of the model is slightly refined (compare with [18]) with the use of experimental data [30] for the carbon dissolution energies (see Appendix).

When cooling, the short-range magnetic order in the α-phase increases, which leads to a decrease in the energy of this phase. In addition, the energy of cementite when cooled decreases faster than the austenite energy. The result is a transition from the γ/α and γ/θ stable equilibria first to the metastable equilibria, and then to their absence while maintaining the α/θ main equilibrium. For qualitative conclusions in the present study, it is only essential that function $f_{\text{eff}}(c)$ is a three-well potential below the critical temperature ($T < T_p$), for which there is no metastable equilibria between austenite and the decomposition products (Fig. 2), as was found before [18].

The density of the elastic energy of the interaction of carbon with stresses is determined by the formula:

$$f_{\text{el.in}}(\mathbf{r}) = \frac{1}{2}\sigma_{ij}(\mathbf{r})\varepsilon_{ij}^{(C)}c(\mathbf{r}), \qquad (2)$$

where $\sigma_{ij}(\mathbf{r})$ are the elastic stresses produced by the growing colony at the point $\mathbf{r}$, $\varepsilon_{ij}^{(C)}$ are deformations created by a single carbon atom. If a carbon atom creates only dilatations

$$\varepsilon_{ij}^{(C)} = \frac{\sqrt{2}}{2}\delta_{ij}\nu^{(C)},$$

Eq. (2) takes the form of

$$f_{\text{el.in}}(\mathbf{r}) = \frac{\sqrt{2}}{4}\nu^{(C)}\sigma_{ii}(\mathbf{r})c(\mathbf{r}).$$

The stresses are determined by the functional of the lattice deformations in the vicinity of the point $\mathbf{r}$

$$\sigma_{ii}(\mathbf{r}) = \frac{1}{L^2}\int K(|\mathbf{r} - \mathbf{r}'|)q[c(\mathbf{r}')]d\mathbf{r}', \qquad (3)$$

where L is the sample size, $q[c(\mathbf{r}')]$ is the function reflecting the presence of the pearlite colony at the point $\mathbf{r}'$ and determined by intrinsic transformation strains e^α and e^θ

$$q[c(\mathbf{r}')] = e^\theta\chi_\theta(\mathbf{r}') + e^\alpha\chi_\alpha(\mathbf{r}'). \qquad (4)$$

where $\chi_\alpha(\mathbf{r}')$ and $\chi_\theta(\mathbf{r}')$ are functions of the shape of ferrite and cementite precipitates, which we define by the Heaviside's functions: $\chi_\alpha(\mathbf{r}') = h[c(T_0) - c(\mathbf{r}')]$ and $\chi_\theta(\mathbf{r}') = h[c(\mathbf{r}') - c(T_1)]$.

The deformations e^α and e^θ will be considered as scalars associated with the change in composition:

$$e^{\alpha(\theta)} = \kappa(c_{a(\theta)}^e - c_0),$$

where $\kappa \equiv \nu^{(C)}$ is the concentration coefficient of the lattice volumetric expansion, c_0 is the starting mean carbon concentration, and $c_{a(\theta)}^e$ are the equilibrium carbon concentrations in ferrite and cementite, $c_\alpha^e \approx 0$ and $c_\theta^e = 0.25$.

Function $K(|\mathbf{r} - \mathbf{r}'|)$ is close in meaning to the Green's function known in the theory of elasticity [33], and is taken in the form of $K(r) = K_0[1 + (r/d)^4]^{-1}$ (hereinafter in calculations $d/L = 0.05$). The normal stresses stretch the γ-phase lattice near ferrite and compress it near cementite; therefore, in this case

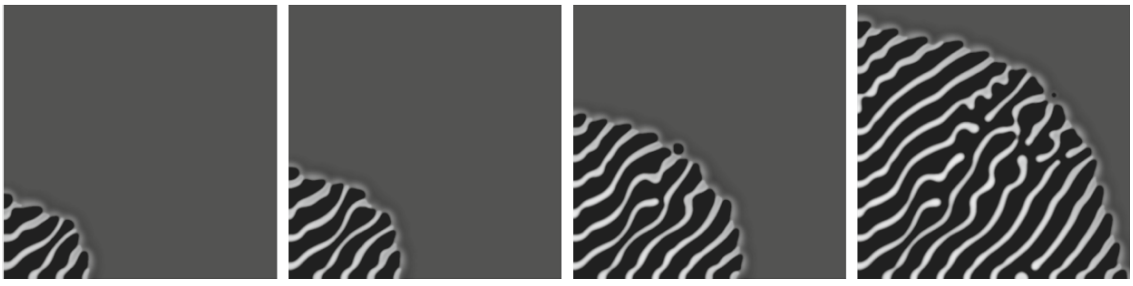

Fig. 4. Kinetics of the pearlite transformation when normal stresses are taken into account; $T = 900$ K, $c_0 = 0.06$, $(d/L)^2K_0 = 1.9$ eV/at.

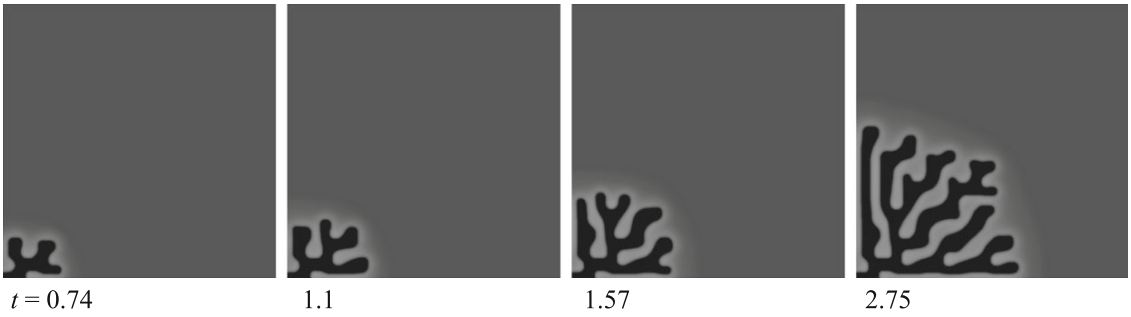

Fig. 5. Branching of ferrite when normal stresses are taken into account; $T = 900$ K, $c_0 = 0.06$, $(d/L)^2K_0 = 0.5$ eV/at.

$K_0 > 0$. On the contrary, the choice of $K_0 < 0$ corresponds to the tangential stresses. The simple model under consideration does not allow us to take these stresses together. However, given that normal stresses prevail at the ends of the colony and tangential stresses may play a role near the front of the colony, their effect on the growth of the colony can be investigated independently.

Stresses in the bulk of the colony are excluded from consideration, since they have an insignificant effect on the diffusion of carbon, which is small in the bulk of the colony, since $D_\theta/D_\gamma \ll 1$ and $c_\alpha^e \ll 1$. However, we will take into account that the stress sign changes to the opposite when passing the colony interface; therefore, in determining the contribution to the free energy functional $F_{\text{el.in}}$, we introduce function $w(c)$, which is converted to zero in α and θ phases:

$$w(c) = h[c - c(T_0)]h[c(T_1) - c],$$

where $h(x)$ is the smoothed Heaviside function. Then $F_{\text{el.in}}$ assumes a form similar to the Kawasaki functional, which was previously used to describe patterns in various systems [34]:

$$F_{\text{el.in}} = \iint c(\mathbf{r})w[c(\mathbf{r})]K(|\mathbf{r} - \mathbf{r}'|)q[c(\mathbf{r})]d\mathbf{r}'d\mathbf{r}. \qquad (5)$$

To describe the evolution of the system, we use the standard diffusion equation [35]:

$$\frac{\partial c}{\partial t} = -\nabla \mathbf{I}, \quad \mathbf{I} = -\frac{D(c)}{kT}c(1-c)\nabla\left(\frac{\delta F}{\delta c}\right). \qquad (6)$$

The diffusion coefficient $D(c)$ is chosen depending on the concentration [18] and takes the values of $D_{\alpha(\gamma,\theta)}$ in the volume of the corresponding phases.

SIMULATION RESULTS AND DISCUSSION

The simulation was carried out on a square grid of 800 × 800 with mirror-symmetric boundary conditions [36] by the Runge–Kutta method. Time t is given in dimensionless units L^2/D_α, where L is the square side size. Different levels of carbon concentration are indicated by gradations of gray color (black color corresponds to ferrite, whereas white corresponds to cementite).

Figures 4 and 5 show the calculation of transformation kinetics at $T = 900$ K and different normal stresses σ_n, but in the absence of tangential stresses ($\sigma_\tau = 0$). The initial state was assumed to be homogeneous with a single ferrite nucleus in the corner of the square. If the value of σ_n is higher than the critical value, a pearlite colony more regular than that in [18] is formed and grows (Fig. 4), with the lamellae oriented at a small angle to its front. The temperature of 900 K is above the temperature T_p of the beginning of autocatalysis in

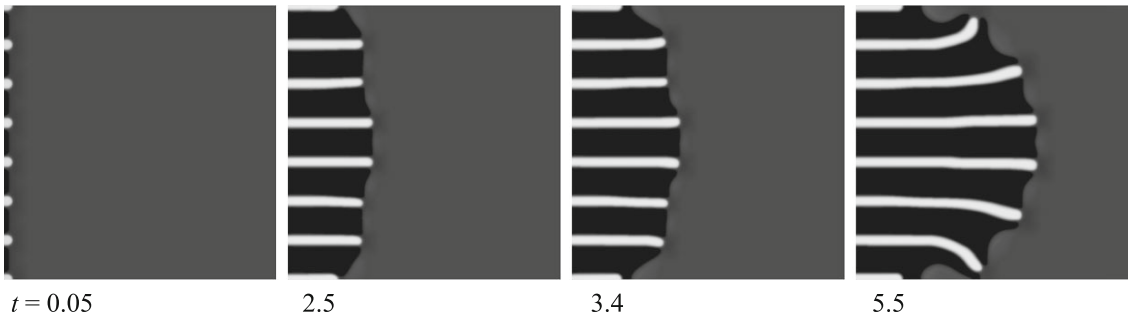

Fig. 6. Kinetics of growth of the pearlite colony when tangential stresses are taken into account; $T = 900$ K, $c_0 = 0.06$, $(d/L)^2 = -0.25$ eV/at.

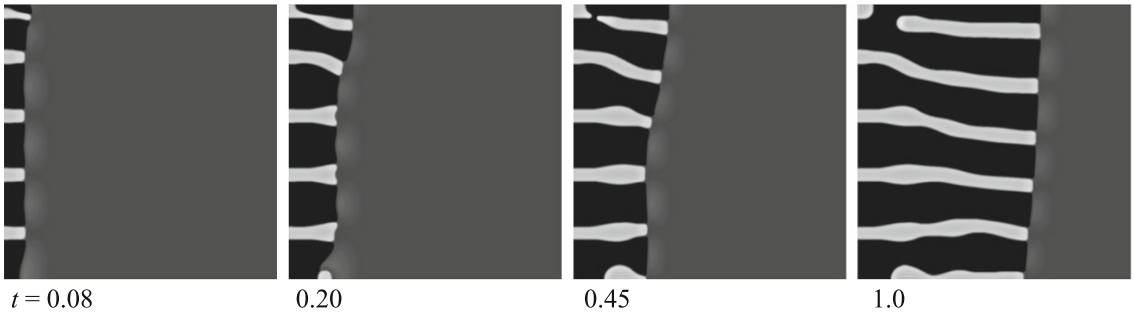

Fig. 7. Kinetics of growth of the pearlite colony when tangential stresses are taken into account; $T = 750$ K, $c_0 = 0.06$, $(d/L)^2 K_0 = -1.9$ eV/at.

the absence of stresses (Fig. 1). Thus, the interaction of carbon with lattice dilatations increases the starting temperature of autocatalysis contributing to the pearlite generation.

With decreasing σ_n at the same temperature, the formation of cementite does not occur, and the branching ferrite structure grows (Fig. 5). Although branching of ferrite is not observed experimentally, the observed tendency can be related to pearlite and bainite transformations. Nowadays, according to the opinion prevailing in the literature, pearlite plates reproduce by side replication [1, 2, 37], which corresponds to the autocatalytic scenario in our model. However, in the Hillert experiments, branching multiplication was observed [24]. In addition, the advance growth of plates of one of the species was observed [38], and in [16] the advancing growth of the cementite plate was obtained numerically when stresses were taken into account. Moreover, when discussing the morphology of the ferrite constituent of bainite, Bhadeshia reports that the ferrite plates are not isolated, but are connected by bridges in the third dimension [39]. The mechanism of reproduction of ferrite plates of bainite remains unclear. It is believed that carbon diffusion can play a role in their nucleation, but in the same time the appearance of cementite is a secondary process.

From a mathematical point of view, the branching of ferrite (Fig. 5) is explained by the decrease in the effective surface energy of ferrite during the segregation of carbon near the interphase. A similar effect was predicted and experimentally confirmed [40–42] for the case when the grain structure is ground by the impurity segregation at the grain boundaries. In [43], the Weissmuller effect was generalized to interphases, leading to the appearance of equilibrium disperse structures. In Figure 5, lattice dilatations provide an energy advantage for retaining carbon near ferrite. Thus, the observed picture is qualitatively similar to the Weissmuller effect and the predictions of the model reported in [43].

When $\sigma_n = 0$, the decomposition develops according to the classical scenario of ferrite precipitation growth [27], and the corresponding calculations are not given here.

To determine the role of tangential stresses σ_τ, the colony growth was simulated when starting from a homogeneous state with a chain of equidistantly arranged ferrite and cementite precipitates at the grain boundary (the position of which coincides with the boundary of the calculated region) at $\sigma_n = 0$. The autocatalytic appearance of such a chain of precipitates on the grain boundary is possible when acceleration of the carbon diffusion on the grain boundary takes place in comparison with the volume of austenite [15].

It is clear from Fig. 6 that at $T = 900$ K even small σ_τ maintain a stable growth of the colony, so that the

lamellae are oriented along the normal to the front. At the same time, a simplified statement of the problem with a separate description of the normal and tangential stresses does not allow us to consider the generation of new lamellae in this case. Figure 7 shows the growth of the colony in the presence of σ_τ at a lower temperature ($T < T_p$), when autocatalytic nucleation of new plates occurs according to the mechanism reported in [18]. In this case, when passing to the steady growth mode, an optimal interplanar distance is revealed; in the transitional stage, oscillation of the width of the plates can take place.

CONCLUSIONS

The interaction of carbon in austenite with lattice dilatations created by the growing pearlite colony stabilizes the colony growth leading to regular decomposition morphologies. In this case, the normal stresses at the ends of the colony increase the temperature of the beginning of the pearlite transformation, and the tangential stresses ensure the stability of the front of the colony. Thus, the acceleration of diffusion at the front of the colony is not a prerequisite for pearlite transformation. The observed mechanism of ferrite branching due to the tendency of carbon segregation near the austenite/ferrite interphase can be related both to pearlite and bainite transformation.

ACKNOWLEDGMENTS

The author thanks Yu.N. Gornostyrev, who suggested the topic of the study.

This work was carried out within the framework of the State Assignment of the Federal Agency of Scientific Organizations of the Russian Federation (topic "Magnet," no. 01201463328).

APPENDIX

MODEL PARAMETRIZATION

The phase energies were calculated using experimental data for the carbon dissolution energies [30], which, in contrast to those given in [18, 27], take into account the temperature dependence: $\tilde{\varepsilon}^{bcc}_{FM(PM)} = \varepsilon^{bcc}_{FM(PM)} - \lambda_\alpha\tau$, $\tilde{\varepsilon}^{fcc}_{FM(PM)} = \varepsilon^{fcc}_{FM(PM)} - \lambda_\gamma\tau$, $\tau = T/T_c$, $\varepsilon^{bcc}_{FM} = 1.1$, $\varepsilon^{bcc}_{PM} = 1.1$, $\varepsilon^{fcc}_{FM} = -0.22$, $\varepsilon^{fcc}_{PM} = +0.38$, $\lambda_\alpha = 0.46$, $\lambda_\gamma = 0.14$ eV/at, $T_c = 1043$ K. These parameters agree with the previous ones near $T \sim 1000$ K, which is in the range of pearlite temperatures.

The carbon mixing energies were assumed to be independent of the magnetic state, $\nu_\alpha = 6$, $\nu_\gamma = 1$ eV/at [44]. The deviation of the free energy of cementite from the free energy of α-Fe was determined by the formula $\Delta f_{\alpha\theta} = b_0 + b_1\tau + b_2\tau^2$, where $b_0 = 0.09$, $b_1 = -0.13$, and $b_2 = 0.04$ eV/at [30, 32]. The T_1 line of the phase diagram, which describes the condition of loss of stability $\gamma \to \theta$ at a constant carbon concentration is shifted to the left (compare [18]) for a qualitative account of the influence of stresses on the nucleation of cementite near ferrite. Herewith, the fact was taken into account that at $c \approx 0.10$ austenite is not observed experimentally [45]. The carbon diffusion coefficients in the phases were chosen $D_\alpha/D_\gamma = D_\gamma/D_\theta = 10$ in qualitative agreement with the data [46, 47]. The parameter k_c, which determines the width of the interface, was determined from the condition of $k_c^2/(kTL^2) \approx 7 \times 10^{-4}$ [48], from which it is possible to estimate the sample size $L \approx 1$ μm.

We also estimate the maximum possible value of coefficient K_0, which determines the magnitude of stresses. The elastic energy from Eqs. (2) and (3) is roughly estimated as $f_{\text{el.in}} \sim (\sqrt{2}/4)K_0\kappa^2 c_0(c_{\text{col}} - c_0)(d/L)^2$, where c_{col} is the carbon concentration in the colony (in ferrite or cementite). On the other hand, the energy associated with the lattice dilatations in the notations of [27] is $f_\nu = A_\nu e_\nu^2/2$, where $A_\nu = 20$ eV/at, and we take $e_\nu = \kappa(c_{\text{col}} - c_0)$ for dilatation. This implies:

$$K_0 \approx A_\nu \frac{\sqrt{2}}{2}\frac{(c_{\text{col}} - c_0)}{c_0}\left(\frac{L}{d}\right)^2. \quad (7)$$

The values of K_0 used in the calculations assume partial relaxation of stresses and are, therefore, chosen to be substantially lower than this estimation.

REFERENCES

1. V. M. Schastlivtsev, D. A. Mirzaev, and I. L. Yakovleva, *Pearlite in Carbon Steels* (UrO RAN, Yekaterinburg, 2006) [in Russian].
2. R. Abbaschian and R. Reed-Hill, *Physical Metallurgy Principles, SI Version* (Cengage Learning, Boston, 2009).
3. M. D. Graef, M. V. Kral, and M. Hillert, J. Met. **58**, 25 (2006).
4. Fu-Wen Ling and D. E. Laughlin, Met. Trans. A **10**, 921 (1979).
5. A. T. Adorno, A. V. Benedetti, R. A. G. da Silva, and M. Blanco, Eclet. Quim. **28**, 33 (2003).
6. A. Das, W. Gust, and E. J. Mittemeijer, Mater. Sci. Tech. **16**, 593 (2000).
7. H. Ramanarayan and T. Abinandanan, Acta Mater. **52**, 921 (2004).
8. A. V. Ponomareva, Yu. N. Gornostyrev, and I. A. Abrikosov, J. Exp. Theor. Phys. **120**, 716 (2015).
9. C. Zener, Met. Technol. **1**, 1 (1946).
10. M. Hillert, Jemkontorets Ann. **141**, 757 (1957).
11. D. Turnbull, Acta Met. **3**, 55 (1955).
12. B. E. Sundquist, Acta Met. **16**, 1413 (1968).
13. A. Yamanaka, T. Yamamoto, T. Takaki, and Y. Tomita, in *Proceedings of the 4th International Conference on*

Multiscale Materials Modeling MMM'2008, Florida, USA, 2008.

14. V. G. Vaks and A. Yu. Stroev, J. Exp. Theor. Phys. **107**, 90 (2008).
15. V. G. Vaks, A. Yu. Stroev, V. N. Urtsev, and A. V. Shmakov, J. Exp. Theor. Phys. **112**, 961 (2011).
16. I. Steinbach and M. Apel, Acta Mater. **55**, 4817 (2007).
17. A. Hultgren, Trans. ASM **39**, 915 (1947).
18. I. K. Razumov, Yu. N. Gornostyrev, and M. I. Katsnelson, Phys. Rev. Appl. **7**, 014002 (2017).
19. I. K. Razumov, Russ. J. Phys. Chem. A **83**, 1682 (2009).
20. I. K. Razumov, Yu. N. Gornostyrev, and M. I. Katsnelson, Phys. Met. Metallogr. **118**, 362 (2017).
21. X. Zhang, T. Hickel, J. Rogal, S. Fähler, R. Drautz, and J. Neugebauer, Acta Mater. **99**, 281 (2015).
22. K. Ankit, R. Mukherjee, T. Mittnacht, and B. Nestler, Acta Mater. **81**, 204 (2014).
23. C. S. Smith, Trans. Am. Soc. Metals **45**, 533 (1953).
24. M. Hillert, in *Decompositionof Austenite by Diffusional Processes,* Ed. by V. F. Zackay and H. I. Aaronson (Interscience, New York, 1962), p. 197.
25. S. A. Hackney and G. J. Shiflet, Acta Mater. **35**, 1007 (1987).
26. B. Ya. Lyubov, *Kinetic Theory of Phase Transformations* (Metallurgiya, Moscow, 1969, Amer. Publ., New York, 1978).
27. I. K. Razumov, D. V. Boukhvalov, M. V. Petrik, V. N. Urtsev, A. V. Shmakov, M. I. Katsnelson, and Yu. N. Gornostyrev, Phys. Rev. B **90**, 094101 (2014).
28. J. S. Smart, *Effective Field Theories of Magnetism* (Saunders, London, 1966).
29. I. K. Razumov, Yu. N. Gornostyrev, and M. I. Katsnelson, J. Phys.: Condens. Matter **25**, 135401 (2013).
30. B. M. Mogutnov, I. A. Tomilin, and L. A. Shvartsman, *Thermodynamics of Iron-Carbon Alloys* (Metallurgiya, Moscow, 1972) [in Russian].
31. J. S. Darken and R. W. Gurry, J. Met. **3**, 1015 (1951).
32. A. Dick, F. Körmann, T. Hickel, and J. Neugebauer, Phys. Rev. B **84**, 125101 (2011).
33. T. Mura, *Micromechanics of Defects in Solids* (Martinus Nijhoff, Dordrecht, Boston, Lancaster, 1987).
34. C. B. Muratov, Phys. Rev. E **66**, 066108 (2002).
35. J. W. Cahn and J. E. Hilliard, J. Chem. Phys. **28**, 258 (1958).
36. K. G. F. Janssens, D. Raabe, E. Kozeschnik, M. A. Miodovnik, and B. Nestler, *Computational Materials Engineering* (Elsevier, Amsterdam, 2007).
37. K. N. Tu and D. Turnbull, Acta Metall. **17**, 1263 (1969).
38. R. F. Mehl and W. C. Hagel, Prog. Metal. Phys. **6**, 74 (1956).
39. H. K. D. H. Bhadeshia, *Bainite in Steels* (IOM Commun., London, 2001).
40. J. Weissmuller, Nanostruct. Mater. **3**, 261 (1993).
41. E. Botcharova, J. Freudenberg, and L. Schulz, Acta Mater. **54**, 3333 (2006).
42. J. R. Trelewicz and C. A. Schuh, Phys. Rev. B **79**, 094112 (2009).
43. I. K. Razumov, Phys. Solid State **56**, 780 (2014).
44. H. K. D. H. Bhadeshia, J. Mater. Sci. **39**, 3949 (2004).
45. V. G. Vaks and K. Yu. Khromov, J. Exp. Theor. Phys. **106**, 265 (2008).
46. *Diffusion in Solids Metals and Alloys, Landolt-Börnstein New Series* (Springer, Berlin, 1990), Vol. III/26.
47. B. Ozturk, Solid State Ionics **12**, 145 (1984).
48. S. Kartha, J. A. Krumhansl, J. P. Sethna, and L. K. Wickham, Phys. Rev. B **52**, 803 (1995).

Translated by V. Avdeeva